POW-GEN3—High-Resolution General Purpose Powder Diffractometer
Conceptual Design Study

J. P. Hodges and R. K. Crawford – 6/01/00

EXECUTIVE SUMMARY

This preliminary conceptual design study for POW-GEN3 is a response to the November, 1998, Instrument Oversight Committee (IOC) request that

"…the SNS should immediately begin work on the conceptual design for … a third generation powder diffractometer with a resolution $\Delta d/d$ of $\sim 1\times10^{-3}$ at 90°"

"The powder diffractometer design presented by the crystallography working group is truly a significant step forward."

"The design should incorporate out-of-plane detectors at 90° for special environments and the resolution should be less than 1×10^{-3} for all angles from back scattering to 90°."

Third Generation Diffractometer Concept

Previous TOF diffractometers used detector "banks" at a few angles, along with a broad wavelength range to produce a limited number of data sets of intensity vs wavelength at these few effective scattering angles. A new idea due to Paolo Radaelli proposes the use of wide angular coverage and full 60-Hz operation to collect a single data set of intensity *vs* angle and time-of-flight. These data would then be combined "appropriately" after-the-fact to produce a single data set with intensity as a function of d-spacing to be used in Rietveld refinement.

This new data collection/analysis concept can be applied to any detector geometry. However, it appears optimally suited to a continuous detector locus, with this locus chosen to optimize the resolution as a function of d-spacing.

Preliminary Instrument Parameters

This preliminary concept for an instrument meeting these IOC requirements has the following basic instrument parameters:

~60 m moderator-sample distance

1-6 m sample-detector distance

sample size ~5 mm diameter × ~20 mm tall

10°-170° continuous detector coverage, with out-of-plane detectors at all angles

~4 steradian detector coverage

curved guide, ~1.5 cm wide and ~3 cm tall

2 bandwidth-limiting choppers and an optional T_0 chopper

Work supported in part by the U. S. Department of Energy, BES, contract No. W-31-109-ENG-38.

Instrument Capabilities

POW-GEN3 will be an extremely versatile general purpose diffractometer useful for a wide range of structural studies. It can cover d-spacings from ~0.5 Å or less to over 20 Å in a single measurement, and is capable of collecting typical Rietveld statistics in ~ 10 minutes from a 0.6 cm^3 sample with <0.1% resolution at short d-spacings and <1% resolution for nearly all d-spacings of interest. Alternatively, much of this resolution can be traded for intensity, making it possible to make measurements in << 5 minutes with still quite good resolution. The adjustable bandwidth-limiting choppers allow large variations in the incident wavelengths and pulse repetition rate. Insertable guide sections and the ability to trade resolution for intensity at the analysis stage allow the users great latitude to optimize the data range, resolution, and statistical precision for each particular experiment.

Major Questions

Although many of the instrument parameters have been at least partially optimized, as described in this document, a number of significant questions remain to be answered. These include

What should be the refined performance specifications for the design of this instrument?

What is the optimal bandwidth?

How should the detector locus be optimized?

What is the optimal combination of out-of-plane detector coverage, sample height, and vertical guide gain?

What detector technology would permit cost-effective coverage of the desired detector locus and detector area?

How can the large data sets be handled?

Next Steps

In order to answer many of these questions it will be necessary to further develop and benchmark the hybrid Monte Carlo-analytical simulation capabilities. Benchmarking will be performed against full Monte-Carlo codes and real diffraction experiments. Rietveld analysis codes then need to be modified to work with single wide-angle data sets of the form that would be generated by this instrument. The relative merits of this concept can then be evaluated by analyzing simulated data sets to explore the range of scientific capabilities of such an instrument. In a limited manner, the narrow bandwidth wide angular coverage concept can be applied to experiments performed on diffractometers such as GLAD at IPNS. This can provide valuable proof-of-concept and data analysis information.

In parallel with these activities, a vigorous program of detector and data acquisition R&D will be essential to achieve the desired instrument specifications and performance.

It will be essential to establish an Instrument Advisory Team (IAT) for this instrument as soon as possible, and to involve this team closely in making the scientific choices necessary for full instrument optimization.

DETAILED DISCUSSION

Contents

1 Instrument Description

In November, 1998, the SNS Instrument Oversight Committee (IOC) recommended five instruments for immediate attention of the design team. (IOC Report – www.ornl.gov/jins/ioc) Among these recommendations was the following statement:

" the SNS should immediately begin work on the conceptual design for … a third generation powder diffractometer with a resolution $\Delta d/d$ of $\sim 1 \times 10^{-3}$ at 90°". "… the design should incorporate out-of-plane detectors at 90° for special environments …".

The IOC went on to say:

"The powder diffractometer design presented by the crystallography working group is truly a significant step forward."

Given these statements, it is important to understand just what is represented by this "third-generation" powder diffractometer concept.

Third Generation Powder Diffractometer Concept

Previous time-of-flight (TOF) powder diffractometers used a few scattering angles, with detectors grouped into banks about these angles. These instruments depended on the use of a broad wavelength range, so that most of the d-spacings of interest could be covered in a single bank. Second generation powder diffractometers expanded the angular coverage both in-plane and azimuthally about the beam, but still maintained the detector bank concept with data reduced effectively to a few scattering angles.

The third-generation concept is based on the idea of Paolo Radaelli at ISIS to use a narrower wavelength bandwidth and make use of wide angular coverage to collect data over all the d-spacings of interest. This narrower bandwidth can be matched to a 60-Hz pulsed source where bandwidth is limited by frame-overlap considerations.

The real breakthrough in this concept lies in the philosophy for data collection and analysis rather than in any specific instrument design. Up to now, the usual case has been to collect a data set for each detector bank. Depending on the scattering angle to each bank, these data sets can cover small d-spacings at high resolution to a wide d-spacing range at low-resolution. This discrete banks method is illustrated in Figure 1 by the dashed lines. The dashed lines show the d-spacing coverage for a typical set of banks. As a consequence of significant resolution differences between each of the banks, the individual data sets cannot be combined usefully into a single histogram.

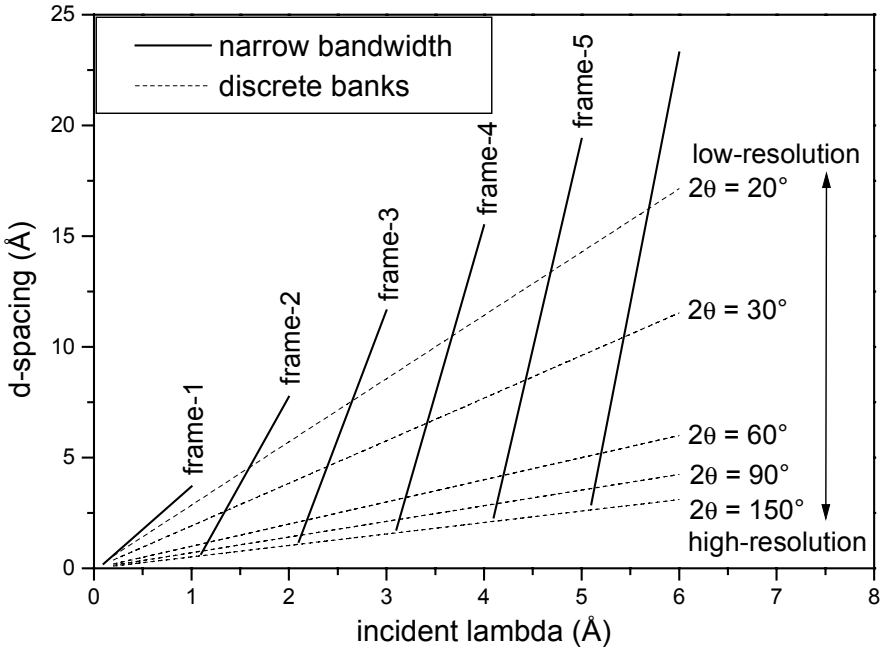

Figure 1. Representation of the d-spacing-lambda space coverage for both narrow bandwidth and discrete detector banks TOF diffractometers. The 2θ values indicate the scattering angle for each detector bank and comprise a typical set for a diffractometer.

In the new concept a data set of intensity *vs* angle and time-of-flight would be collected for all detector angles for each wavelength band (frame) being used. This narrow bandwidth (NBW) method is represented in Figure 1 by the solid lines. Each solid line shows the d-spacing coverage achievable for a given wavelength band (the wavelength bands have been assigned according to which time frame they appear in for a 60 m flight path diffractometer). Using an appropriately optimized detector locus with this NBW approach, the individual data sets for different frames can be combined to yield a single histrogram of very wide d-spacing converage. Importantly, at this data reduction stage resolution can be traded for intensity.

Such an instrument with wide and continuous detector coverage with a user-selectable choice of wavelengths for data collection and complete freedom in selection of the subset of the data to be included in the analysis offers enormous flexibility. This will enable the users to optimize the instrument and data analysis configurations for an extremely broad variety of experiments.

SNS Instrument

This concept of a continuous detector locus optimized to provide the desired resolution profile, with a high degree of flexibility in the data collection and analysis parameters, is the basis for the conceptual design being developed to meet the IOC recommendation. The current status of this concept is outlined here.

So far, it has been assumed that this instrument would view a poisoned ambient water moderator, and should view this moderator normally to minimize neutron path length

uncertainties. The requirement for 0.1% resolution coupled with the pulse width from such a moderator dictates the incident path length, and the angular uncertainties dictate the sample-detector distances as a function of scattering angle.

Wavelength Bandwidth

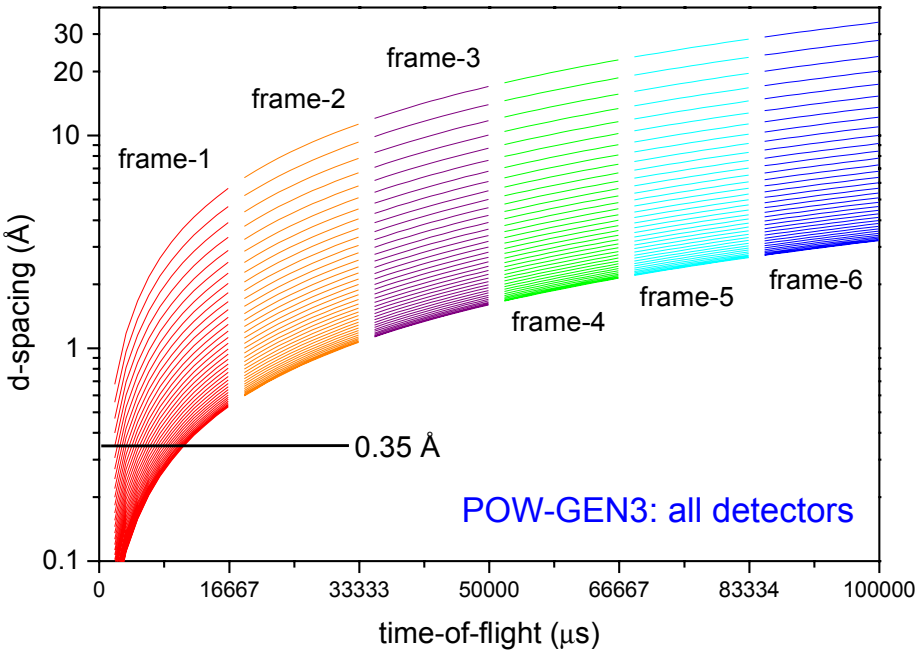

Figure 2. The d-spacing range surveyed by POW-GEN3 for each of the ~1 Å bandwidth frames.

At 60 m on a 60 Hz source the wavelength bandwidth unobstructed by frame overlap is ~1 Å. A combination of bandwidth-limiting choppers is required to restrict wavelengths incident on the sample to within this ~1 Å band. These choppers are rephased when it is desired to utilize a similar band centered at a different wavelength. The d-spacing coverage of the first six bands are show in Figure 2. If desired, the system of choppers can eliminate some of the pulses completely to provide a source effectively operating at a lower repetition rate.

An exciting option, is to have the bandwidth choppers operated at a speed different to the source frequency, for example 80 Hz could yield frame-1 followed by frame-5 followed by frame-3 and 1-5-3-1... This commensurate chopper mode of operation is potentially very powerful, since it allows the experimenter several chopper settings of speed and phase to operate POW-GEN3 and each setting has a different weighting between incident intensity and d-spacing range covered. Once refined, this mode of operation would likely become the standard mode of operation of POW-GEN3.

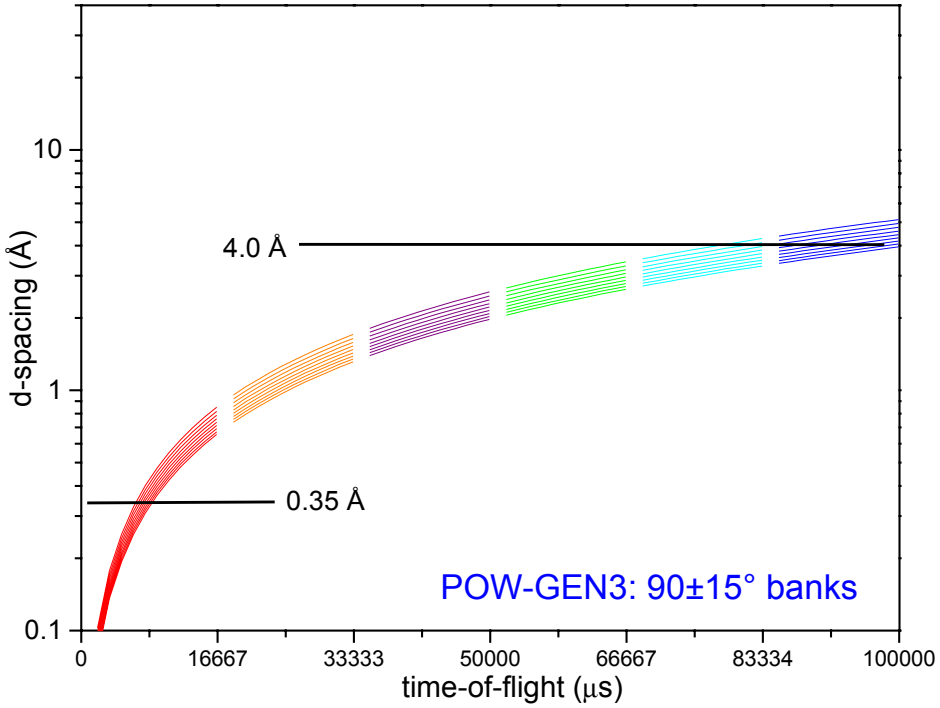

Figure 3. The d-spacing range surveyed by the pseudo-90° detector banks of POW-GEN3.

The application of the NBW technique must also be evaluated for special environment experiments, e.g. use of hydrostatic pressure cell, when only detectors near 90° scattering angles will be collecting data. In Figure 3 the d-spacing coverage for such an experiment is shown. With a useful d-spacing range of < 0.35 Å to ~4 Å, POW-GEN3 is well matched for studying crystal structure response under applied conditions. The actual d-spacing range measured will be set by having the choppers eliminate pulses or run in commensurate speed mode as described in the previous paragraph.

A very fast alternative mode of operation, which makes more efficient use of the 60 Hz pulsed source, is plausible for experiments where the powder of interest is of known crystal structure (this is generally case for parametric studies). In this mode, the bandwidth choppers are set such that they allow a large wavelength band, e.g. ~6 Å, to pass for each pulse and thus do not prevent frame overlap. The data set collected contains all the reflections that would normally be distributed across several frames all superimposed onto a single frame. Figure 4 shows a simulation of a diffractogram collected by this 'frame-overlap permitted' mode for a 1 gram powder sample of silicon (details of how simulations are performed are given in section 2.2). There appears to be no obstacles preventing the analysis of diffraction data collected in this manner by the Rietveld method. However, this mode of data collection places limits on the amount of jitter and drift allowed between target pulses (the detrimental effects of jitter and drift have not presently been quantitatively assessed).

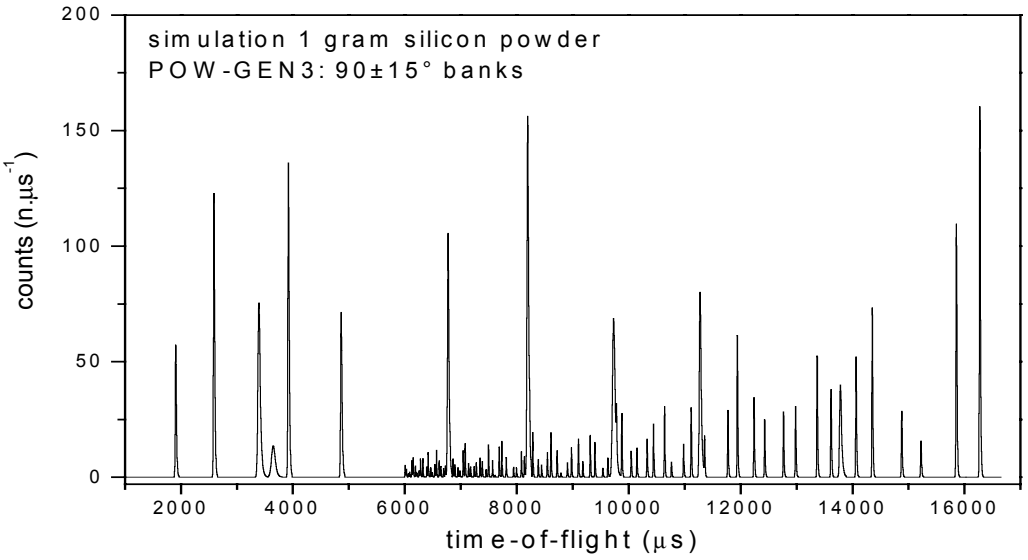

Figure 4. A simulated diffractogram for POW-GEN3 operating in a frame overlap mode.

Detector Coverage

The following equation has been used to provide a simple variable analytical expression to allow the broad effects of detector locus to be explored in Monte Carlo resolution calculations.

$$L_{scat} \approx A + B\sqrt{\cot\theta} \qquad (1)$$

Here A and B are arbitrary constants. Figure 5 shows a typical detector locus produced by this equation.

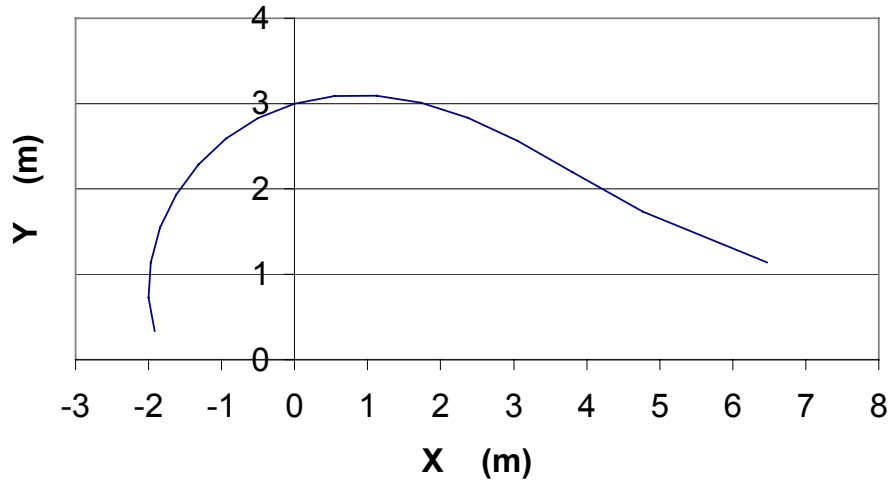

Figure 5. Trial detector locus for resolution calculations. The sample is located at 0,0 and the neutrons are incident from the left along the x-axis.

To achieve both high instrument efficiency and high resolution dictates that POW-GEN3 has large solid angle detector coverage of ~ 4 steradians and that this detector surface is highly pixelated. As a starting point for performance evaluation and detector coverage optimization, an azimuth angular coverage of ±30° at all in-plane scattering angles, 10° - 170°, complemented by increased azimuthal coverage to ±45° for scattering angles 90±15°, along with a pixel size of 40 mm height by 5 mm width, has been assumed. The increased detector coverage at scattering angles near 90° increases the performance for constrained environment experiments. With this preliminary detector angular coverage and pixel size, POW-GEN3 has ~ 240,000 individual pixels (see Figure 6).

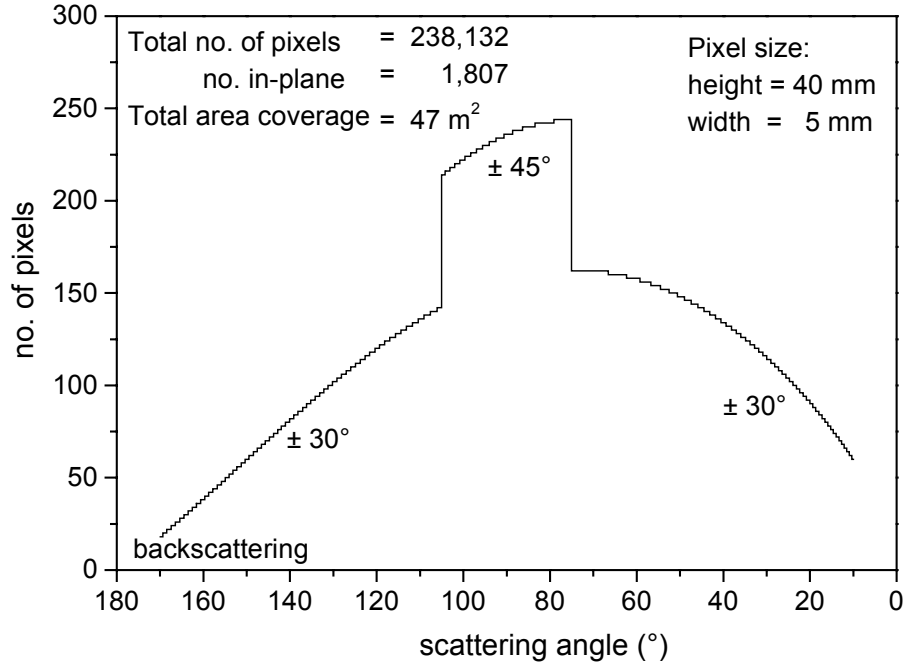

Figure 6. The combined (left and right banks) pixel coverage of POW-GEN3.

Although not included in the performance evaluation of POW-GEN3 presented in this report, increasing the detector coverage at backscattering angles ($2\theta > 130°$) will be advantageous for experiments requiring the highest resolution ($\Delta d/d \approx 0.05\%$), improved statistics of reflections at small d-spacings, the determination of preferred orientation pole figures of textured samples, and pair-distribution function (PDF) analysis.

Because of the long 60 m flight path POW-GEN3 would be housed in a separate building outside the main experiment hall. Figure 7 shows a close-up 3-D model of the powder diffractometer detector geometry as conceived at present. Figure 8 shows a plan view with somewhat greater detail. Table 1 summarizes the parameter specifications based on a preliminary optimization of this instrument.

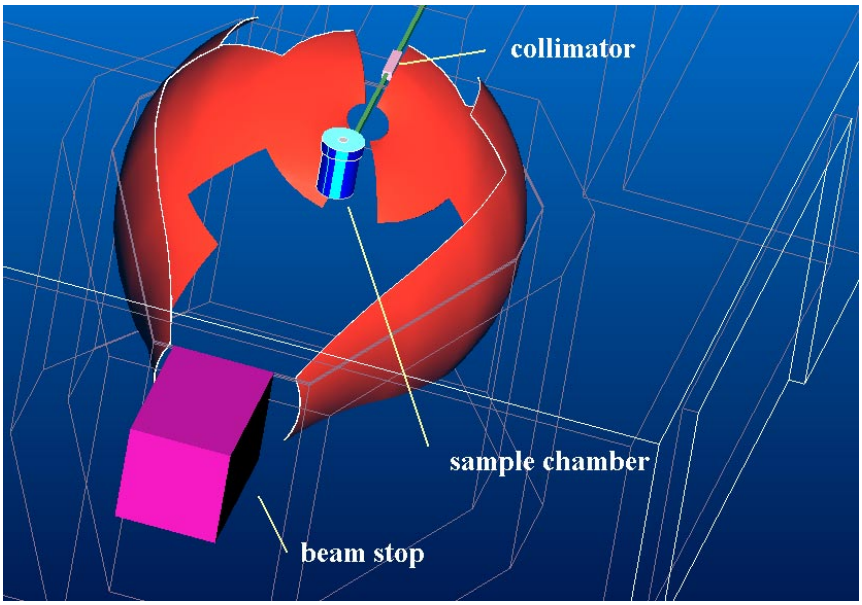

Figure 7. 3-D model of preliminary powder diffractometer concept. The neutron beam is incident from the top. Shielding and building to house the instrument are shown as transparent.

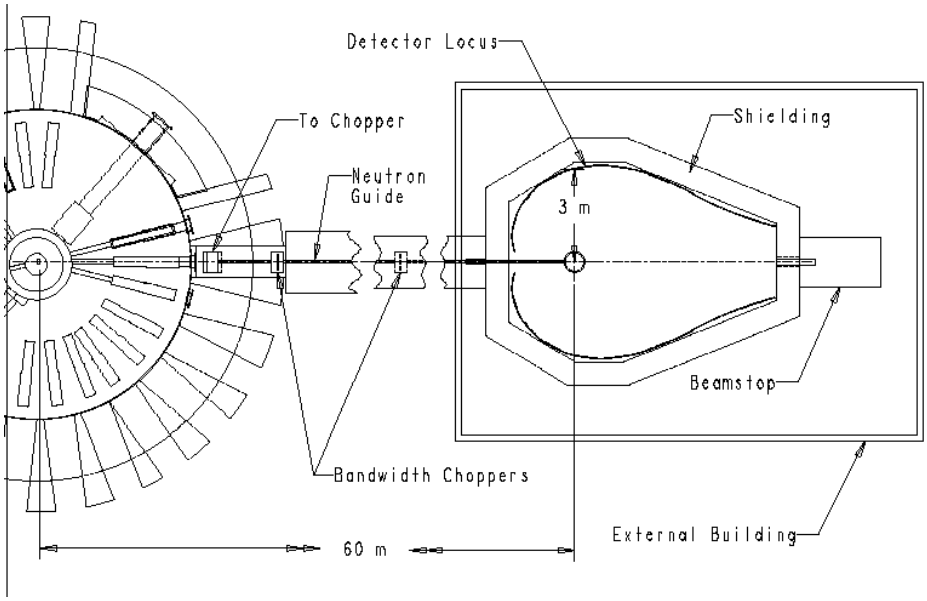

Figure 8. Schematic plan view of the SNS third generation powder diffractometer.

Table 1. Parameters for the powder diffractometer POW-GEN3

Component	Parameter	Value
Moderator	Beam line	8BU
	Moderator	Liquid-H_2O, decoup, pois
	Pulse width	10 μs at 1 Å
Geometry	Source-sample distance	60 m
	Sample-detector distance at 170°	1.9 m
	Sample-detector distance at 90°	3.0 m
	Sample-detector distance at 10°	6.6 m
T_0 chopper (optional)	Type	Horizontal-axis T_0 – 1-blade
	Radius to beam center	250 mm
	Length	300 mm
	Distance from moderator	5.5 m
	Frequency	60 Hz
	Beam width at chopper	~15 mm
	Wavelength range to open or close	0.11 Å @ 60 Hz
Bandwidth chopper #1	Type	Disk
	Radius to beam center	250 mm
	Length	10 mm
	Distance from moderator	7.5 m
	Frequency	10 to 60 Hz
	commensurate mode option:	10 to 90 Hz
	Beam width at chopper	15 mm
	Wavelength range to open or close	0.08 Å @ 60 Hz
Bandwidth chopper #2	Type	Disk
	Radius to beam center	250 mm
	Length	10 mm
	Distance from moderator	20 m
	Frequency	10 to 60 Hz
	commensurate mode option:	10 to 90 Hz
	Beam width at chopper	15 mm
	Wavelength range to open or close	0.03 Å @ 60 Hz
Guide†	Type	Curved
	Radius of curvature	10,809 m
(† *parameters will be optimized further*)	Coating, sides	natural Ni
	Coating, top and bottom	$3 \times \theta_c$ supermirror
	Channel width	15 mm
	Channel height	30 mm
	Moderator-to-guide distance	~8 m
	Moderator to end of guide sides	Adjustable, ≥ 51 m
	Moderator to end of guide top and bottom	Adjustable, ≥ 51 m
	Line-of-sight distance	36 m
	Characteristic wavelength	0.98 Å
	Filling	Evacuated to $<10^{-2}$ torr
Collimation	Near sample	Variable aperture

Table 1 (continued)

Component	Parameter	Value
Beamline shielding	Steel radial thickness around beam	TBD
	Paraffin radial thickness around steel	TBD
	Channel for guide	0.2 m × 0.2 m
	Length	46.5 m
Beam-stop	Steel	TBD
	Paraffin radial thickness around steel	TBD
	Re-entrant hole in steel	0.2 m × 0.2 m × 0.5 m
Sample	Width (maximum beam size)	~10 mm
	Height (maximum beam size)	~30 mm
Detector angular coverage	In-plane	Continuous 10° - 170°
	Out-of-plane	Variable ±30° or ±45°
Detectors	Type	TBD
	Pixel size	40 mm × 5 mm
	Distance from sample	Variable 1 – 6 m
	Solid angle coverage	~4 sr
	Area	~47 m^2
	Number of pixels	~240,000
Data acquisition		standard system
Scattering chamber	Geometry	TBD
	Size	TBD
	Filling, direct beam portion	evacuated to $<10^{-2}$ torr
	Filling, remainder	TBD
	Shielding thickness and composition	TBD
Sample chamber	Geometry	TBD
	Filling	Various, incl. 10^{-6} torr

2 Performance Estimates

Presently the purpose of the curved neutron guide is to prevent direct line of sight to the moderator thus reducing background noise, and permit, on an individual experiment basis, a trade off between modest guide gain (≤ ×4) and resolution. Monte Carlo calculations, which are presented in section 3.3 of this report, show that a curved guide can meet these goals.

For this report calculations that are a hybrid of Monte Carlo ray tracing and analytical approaches are presented for POW-GEN3 based on the instrument parameters specified in Table 1, except that no guide has been assumed, i.e. natural collimation. These performance estimates are justified for POW-GEN3 with a curved guide, since the guide will be able to illuminate the sample at the natural divergence of ~0.8 mrad and a gain of ~1. At present the code which performs the calculations is not able to include neutron guide sections in its' model of the diffractometer. Development of the Monte Carlo ray tracing code to include modeling of neutron guide sections is planned.

2.1 Resolution

In-plane Resolution Calculations

The instrument is assumed to collect data for all neutrons falling within the selected incident bandwidth and scattered into angles covered by the detectors (10°-170°). The detector locus chosen for these calculations is shown in Figure 5. The resolution was determined for every 20th detector lying in the horizontal scattering plane by a simple Monte Carlo ray tracing method. The moderator was modeled as a flat 12 cm high × 10 cm wide surface of even brightness, the sample a 15 mm height × 3 mm diameter cylinder, and the detector pixels each a cylinder of 10 bar He^3 gas of 40 mm height × 5 mm diameter. The detectors are orientated perpendicular to the scattering plane. The total and partial in-plane geometrical resolution functions shown in Figure 9 were determined from distributions of effective path lengths traveled for neutrons ($\lambda = 2.5$ Å) of random origin, scattering and detection locations. Very similar functions are found for neutron wavelengths 0.25 Å < λ < 6 Å.

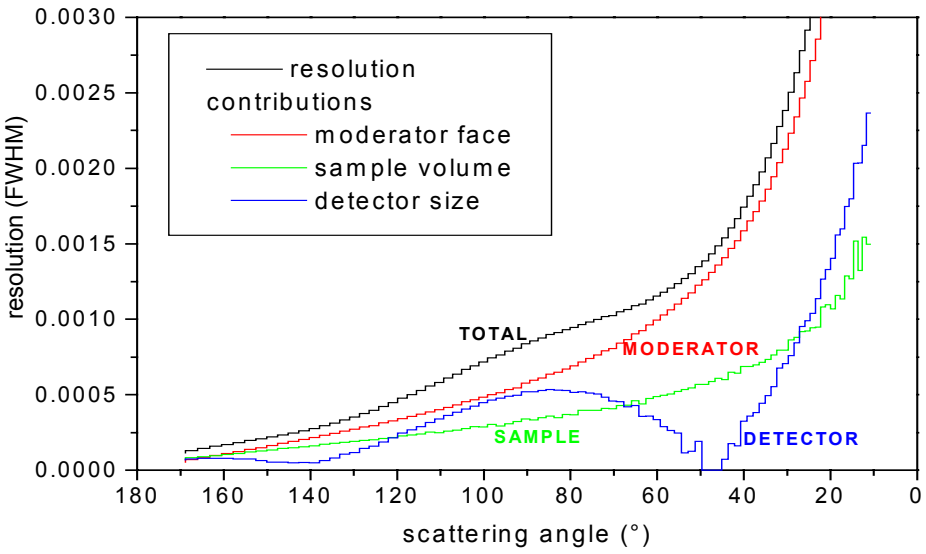

Figure 9. The total and partial in-plane full-width half-maximum (fwhm) geometrical resolution functions determined for the POW-GEN3 concept design by Monte Carlo ray tracing method.

Figure 9 shows that an in-plane instrument resolution of 8.5×10^{-4} at 90° can be achieved with the proposed detector geometry. However, these resolution calculations have not included the moderator pulse shape. Simply taking for an ambient H_2O moderator a fwhm of $\delta t \approx 10$ μs at 1 Å yields a fwhm resolution of 1.1×10^{-3} at 90°.

In Figure 9 the presence of detector focusing can be seen in the detector partial resolution function at scattering angles near 45° and 145°. This focusing occurs because the difference in path lengths between top and middle of a detector pixel is compensated by the associated change in scattering angle. The possible exploitation of this form of detector focusing will be investigated for the optimization of the POW-GEN3 detector surfaces.

Out-of-Plane Effects

Crude analytical approximations have been made to estimate the magnitude of the resolution effects associated with extending the detector bank out of the scattering plane. The geometry used for calculating out-of-plane contributions to the resolution is shown in Fig. 10. In all cases the detector is assumed to form part of a surface of revolution about the beam axis, so that L_{scat} is constant for a given nominal scattering angle 2θ. The simple estimates here suffice only to establish the approximate magnitudes of some of the out-of-plane effects. More accurate estimates and optimizations will be done with the Monte Carlo simulation code being developed.

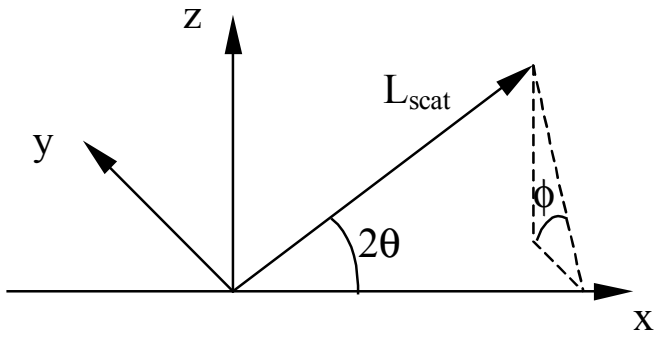

Figure 10. Geometry for discussion of out-of-plane effects. The sample has its long direction along the vertical direction (z).

To first order the variation in θ from one end of the sample to the other end of the sample for given nominal values of θ and ϕ is

$$\delta\theta'_{v1} \approx \frac{H_{samp}}{2L_{scat}} \cos 2\theta \sin\phi \tag{2}$$

giving a fwhm variation of

$$\delta\theta_{v1} \approx \frac{H_{samp}}{3L_{scat}} \cos 2\theta \sin\phi \tag{3}$$

Here the nominal directions of θ and ϕ are based on the line from sample center to detector pixel center, and H_{samp} is the sample height.

A second contribution to the out-of-plane resolution effects comes from the vertical divergence in the incident beam due to the collimation system or guide. This makes another contribution to $\delta\theta$ given approximately by

$$\delta\theta'_{v2} \approx \frac{\alpha_{inc}}{2} \sin\phi = \frac{H_{guide}}{2L_{guide-samp-vert}} \tag{4}$$

where α_{inc} and $\delta\theta'_{v2}$ are the maximum incident beam vertical divergence and the maximum projected contribution of this divergence to the Bragg angle uncertainty.

A third out-of-plane contribution to $\delta\theta$ can arise from the finite size of the detector pixel. This term is highly dependent on the geometry assumed for the detector pixels, and for now it will be assumed that this term is small compared to the other two.

All of these terms contribute in quadrature to the $\delta\theta$ from in-plane resolution effects. The scattered beam and incident beam in-plane terms are

$$\delta\theta_{h1} \approx \frac{1}{2L_{scat}}\left(W_{det}^2 + W_{samp}^2\right)^{1/2} \tag{5}$$

$$\delta\theta_{h2} \approx \frac{W_{guide}}{2L_{guide-samp-horiz}} \tag{6}$$

If we assume that the in-plane divergence effects are reasonably well optimized, then to keep the out-of-plane contribution to the scattered beam divergence small requires $\delta\theta_{v1} \le \delta\theta_{h1}$ or

$$\left|\frac{2H_{samp}}{3}\cos 2\theta \sin\phi\right| \le \left(W_{det}^2 + W_{samp}^2\right)^{1/2} \approx 6\text{ mm} \tag{7}$$

Similarly, to keep the out-of-plane contribution to the incident beam divergence small requires $\delta\theta'_{v2} \le \delta\theta_{h2}$ or

$$\frac{H_{guide}}{L_{guide-samp-vert}}\sin\phi \le \frac{W_{guide}}{L_{guide-samp-horiz}} \tag{8}$$

For $\phi_{max} = \pm 30°$, $\sin(\phi_{max}) = 0.5$ so Eq. (7) gives $H_{samp} \le 18$ mm ($H_{samp} \le 13$ mm when $\phi_{max} = \pm 45°$) and Eq. (8) requires that the incident vertical divergence be limited to twice the incident horizontal divergence.

In addition, there can be a path-length difference associated with the sample height and also with the dimensions of the detector pixel. If the detector pixel is assumed to be small, then this term is roughly

$$\delta L \approx H_{samp}\cos 2\theta \sin\phi \tag{9}$$

To keep the contribution of this term small requires

$$\frac{\delta L}{L} \le \frac{\delta t}{t} \approx 6.6\times 10^{-4} \tag{10}$$

or

$$H_{samp}\cos 2\theta \sin\phi \le 40\text{ mm} \tag{11}$$

This condition is satisfied for all values of θ and ϕ if $H_{samp} \le 40$ mm

Considering all these conditions together implies that the sample height should be no more than ~20 mm and the vertical guide gains should be limited to a factor of ~2 in order to avoid seriously spoiling the resolution of this instrument. A more accurate assessment awaits detailed Monte Carlo simulation of the full 3-D geometry.

2.2 Data Rates

Data rates for POW-GEN3 have been estimated by simulating simple diffraction experiments.

In these calculations a spectrum is simulated for every 20^{th} in-plane detector pixel. The peak profiles are modeled by convoluting the total in-plane geometrical resolution (shown in Figure 9) with moderator peak intensity and shape functions. For both the geometrical resolution and moderator pulse shape, back-to-back exponentials convoluted with a Gaussian function have been used. Using the same function for both instrument resolution and moderator pulse shape, enables asymmetric character in the resolution distribution for an individual detector pixel to be easily convoluted with the moderator pulse shape. Each spectrum is then multiplied by the total number of pixels (in-plane + out-of-plane) at that particular scattering angle (see Figure 6) and further multiplied by 20. Finally, the 90 spectra are combined to yield a single diffractogram of neutron counts vs. d-spacing. In these simulations noise and background are not included at present.

In the above method the resolution function determined for in-plane pixels has been applied to out-of-plane pixels. Since, this is not a valid assumption the results presented here are approximate. More precise calculations that include Monte Carlo simulations of the 3D detector geometry are a primary goal for code development.

Furthermore, in the above method the 90 spectra are combined in their entirety without using a sliding resolution window for discrimination. However, the POW-GEN3 concept calls for such a resolution window at the data reduction stage. Briefly, for each d-spacing point the resolution window selects a subset of pixels that contribute based on each pixel's resolution. By varying the size and d-spacing dependence of the window, POW-GEN3 will be able to perform modest trade between overall resolution and intensity after data collection, thus allowing the experimenter a valuable degree of 'fine-tuning'.

Source

The current SNS baseline plan has a composite H_2O-liquid H_2 moderator at the bottom-upstream (BU) position. The neutronic performance of this proposed composite moderator is being evaluated. However, at present time there is insufficient quantitative information for evaluating a composite moderator - POWGEN3 instrument combination. Therefore, for performance evaluation a poisoned decoupled ambient temperature water moderator and a beam line normal to the moderator surface has been assumed for POW-GEN3. This moderator and beam line configuration will present sharp pulses, high intensities at intermediate d-spacings, and the best possible timing resolution for the instrument.

For the diffraction experiment simulations, the H_2O BU moderator brightness expected for 2 MW operation was used. Figure 11 shows the expected integrated moderator brightness per resolution element as a function of wavelength for this moderator.

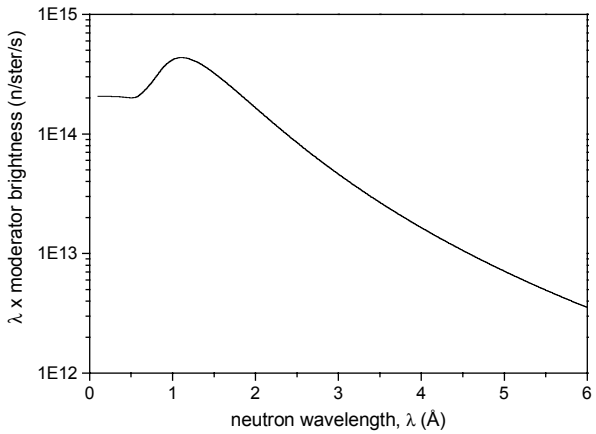

Figure 11. The integrated moderator brightness per resolution element expected for a bottom upstream ambient H_2O moderator at 2 MW operation of SNS.

The moderator pulse shape parameter dependencies for the back-to-back exponential profile function used in the simulations are shown in Figure 12 a). Figure 12 b) shows two example pulse shapes corresponding to neutron wavelengths of 0.85 Å and 1.95 Å. These dependences were determined for a poisoned liquid methane moderator (F moderator at IPNS). The difference in pulse shapes between poisoned liquid H_2O and poisoned liquid methane moderators are of relatively small importance with regard to the overall data collection rates of a diffractometer. The corresponding pulse shape dependencies for a poisoned H_2O moderator is currently being determined from analysis of standard powder diffraction data collected on the POLARIS diffractometer at ISIS.

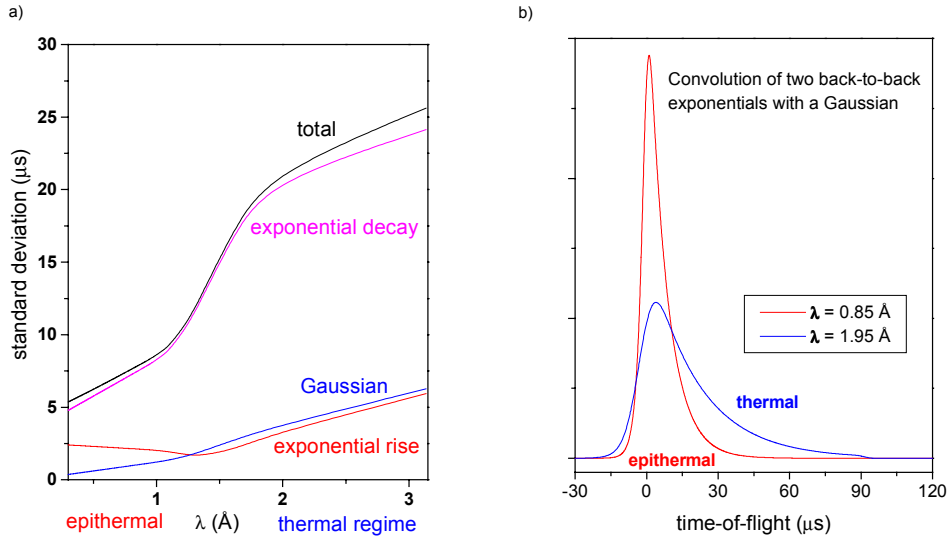

Figure 12. a) Pulse shape parameter dependencies for a liquid (100 K) methane moderator used for simulating diffraction spectra. The pulse profile function has three shape terms, an exponential rise term, an exponential decay term and a Gaussian term. b) Example epithermal (λ = 0.85 Å) and thermal (λ = 0.85 Å) regime pulse shapes produced by the profile function.

Simulation

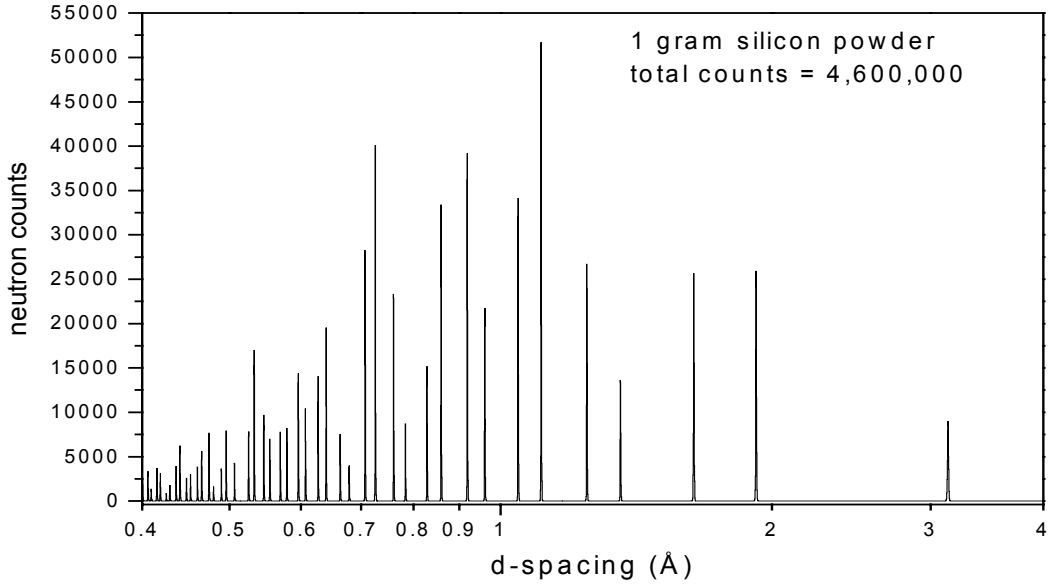

Figure 13. Simulated diffraction profile for 1 gram of silicon powder, 1 min total collection time of frames 1 + 2 (0.3 Å < λ < 2 Å), using the present concept design of POW-GEN3. The d-spacing bin size is $\Delta d/d = 0.2\times10^{-3}$.

For the experiment simulations of POW-GEN3, a detector efficiency equivalent to 1 cm of 10 bar He^3 gas has been assumed. Figure 13 shows a simulation for 1 gram of silicon powder collected using frames 1 and 2 each for 30 s (total collection time = 1 min). With a total count of 4.6×10^6 over ~50 reflections, this can be considered sufficient for precise Rietveld analysis. Typically, samples of interest will possess considerably more complex crystal structures than silicon, therefore for a 0.5 gram sample similar statistics per reflection are expected to be obtained within 8 - 16 mins collection time.

To estimate the maximum instantaneous and maximum time averaged count rates per cm^2 of detector area, a simulation for 1 gram of nickel powder was performed. Figure 14 shows the expected diffractogram for 1 min of collection time. From the individual pixel spectra a maximum instantaneous count rate of 100 $cts.s^{-1}.cm^{-2}$ was determined. This maximum instantaneous count rate is considerably higher than a rate of ~3.5 $cts.s^{-1}.cm^{-2}$ estimated by scaling from the GPPD diffractometer at IPNS [1]. This difference in values is a probably a result of not adjusting for the much higher resolution of POW-GEN3 at the lower scattering angles in the scaling calculations. The maximum time-averaged count rate per cm^2 of detector is estimated to be ~0.01 $cts.pulse^{-1}.cm^{-2}$, the same value was found by scaling estimates [1].

The values for maximum instantaneous and time averaged count rates per cm^2 should be increased by at least a factor of 4 in the cases where the resolution is relaxed and the guide gain is increased. With 47 m^2 of detector coverage area, a time-averaged total data rate of $\sim3\times10^5$ $cts.s^{-1}$ time averaged over the whole detector array is estimated ($\sim1\times10^6$ cts s^{-1} in the relaxed-resolution case).

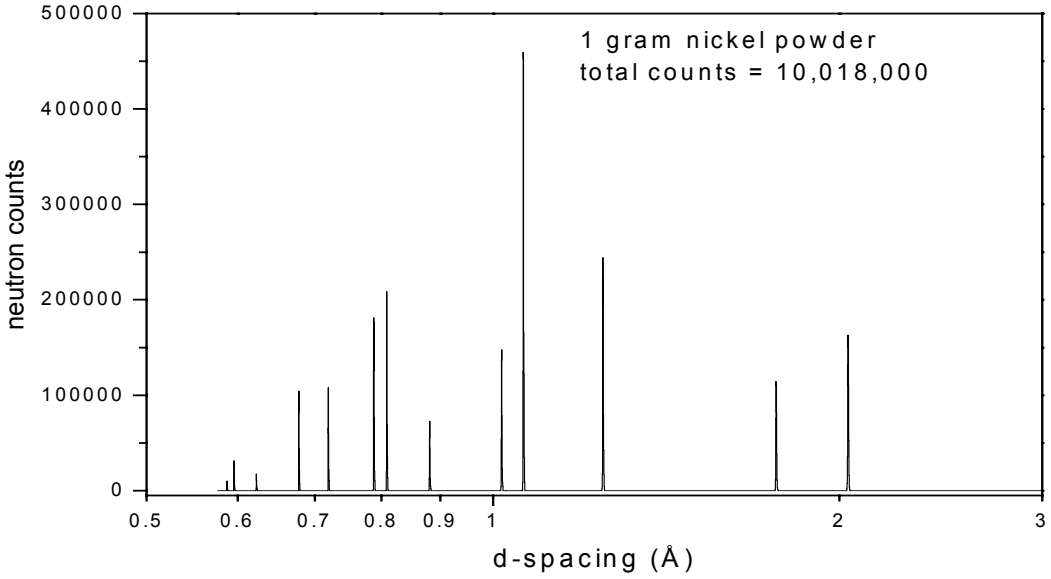

Figure 14. Simulated diffraction profile for 1 gram of nickel powder, 1 min total collection time of frame 2 (1.1 Å < λ < 2 Å). The d-spacing bin size is $\Delta d/d = 0.2\times10^{-3}$.

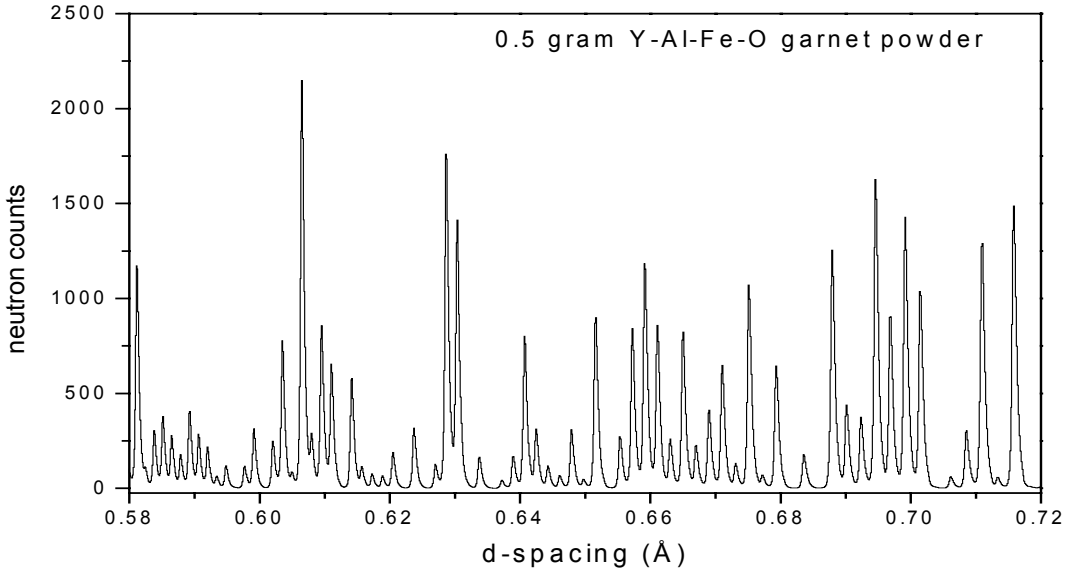

Figure 15. Part of a simulated diffraction profile for 0.5 gram of Y-Al-Fe-O garnet powder, 1 min total collection time of frames 1 + 2. The d-spacing bin size is $\Delta d/d = 0.2\times10^{-3}$.

To gain a more practical impression for the diffraction data that will be collected by POW-GEN3, a simulation for a structurally more complex Y-Al-Fe-oxide garnet powder is shown in Figure 15. Clearly, both the resolution ($\Delta d/d = 1.1\times10^{-3}$) and count rate are high after a collection time of 1 min.

2.3 Performance Discussion

This preliminary performance evaluation using the instrument parameters selected presents the picture of an extremely flexible and capable instrument. Resolutions are quite high, data rates are reasonable, and the dynamic range is outstanding. With this design, resolution can easily be sacrificed when higher data rates are needed for time-dependent studies.

Full optimization of the design for such an instrument will require realistic simulation tools and data analysis codes capable of refining the simulated data sets. It will also be necessary to define further the types of science to be considered as a basis for such an optimization.

3 Preliminary Optimization of Specific Components

3.1 Choppers

A T_0 chopper (optional) is used to cut out the prompt pulse to reduce background, and a series of bandwidth-limiting choppers is required to limit the incident bandwidth to prevent frame overlap, the condition in which fast neutrons from one pulse catch up with slow neutrons from the preceding pulse. To provide maximum flexibility, this series of choppers must be able to select different bandwidths as well as to vary the wavelength at which the incident bandwidth is centered. The requirement to vary the selected bandwidth can be satisfied by using choppers with adjustable openings. This bandwidth can be centered at any wavelength simply by adjusting the phase of the bandwidth choppers. A second chopper, properly positioned and phased, is required to cut out additional neutrons that could contaminate the data. Additional choppers would be needed if wavelengths beyond ~6 Å are to be used.

Preliminary optimization of the chopper locations and speeds was done using a spreadsheet to evaluate the wavelengths for which the chopper system is fully open and the wavelengths for which one or more of the choppers is opening or closing. Table 2 shows the parameters assumed for the choppers, and Tables 2a and 2b show the opening and closing times and wavelengths for each of these choppers for several different choices of chopper phases.

Figure 16 shows a time-distance diagram for POW-GEN3 based on the data in Tables 1-2 for several different choices of chopper phasing. It is evident that for some of these phasing choices the second bandwidth chopper is needed to block unwanted wavelengths (e.g., neutrons from the wrong pulse) that can pass through the first chopper.

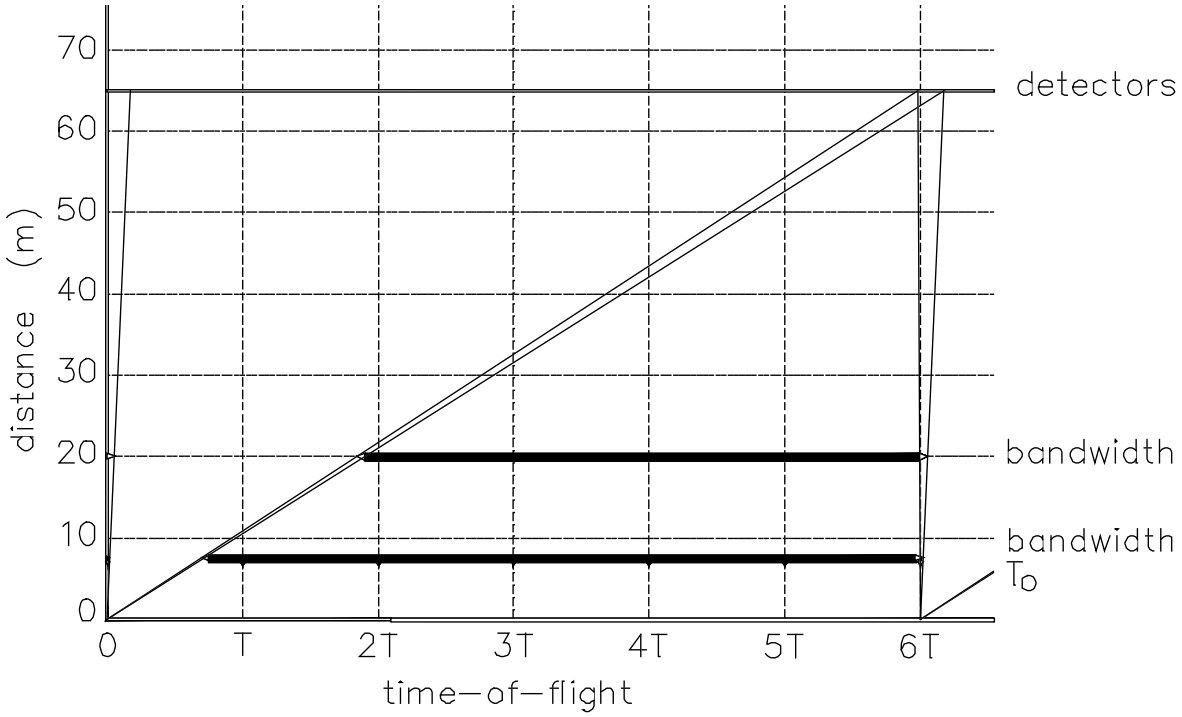

Fig. 16a

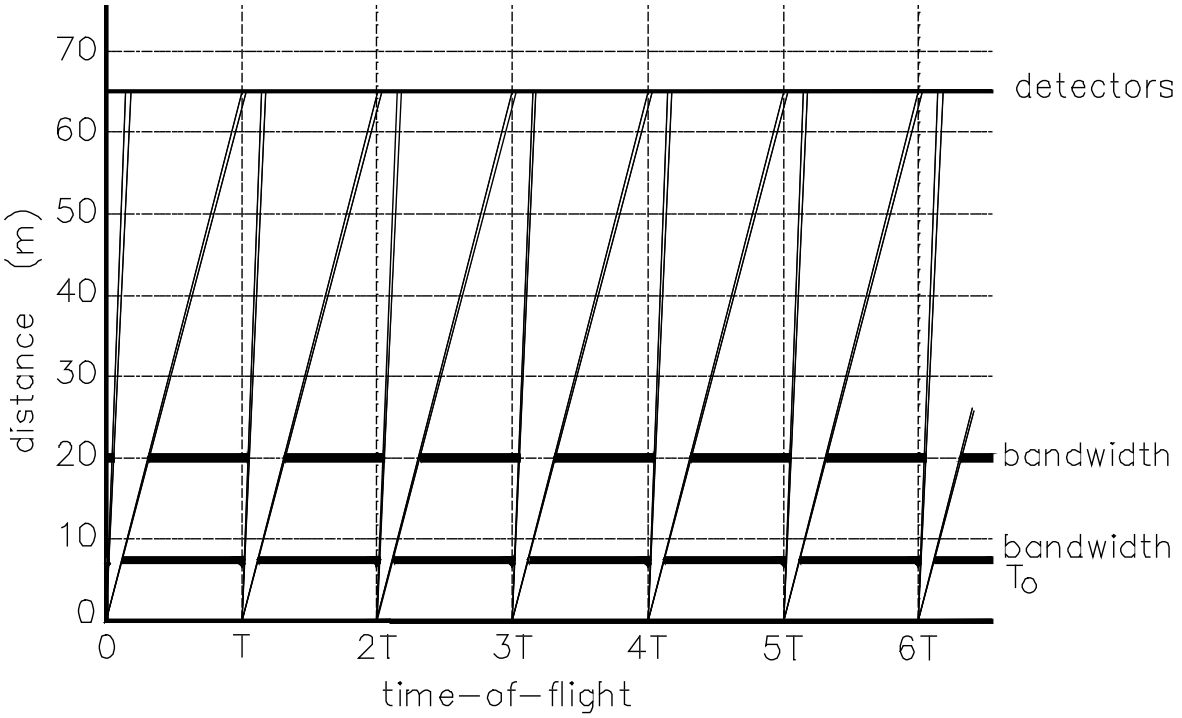

Fig. 16b

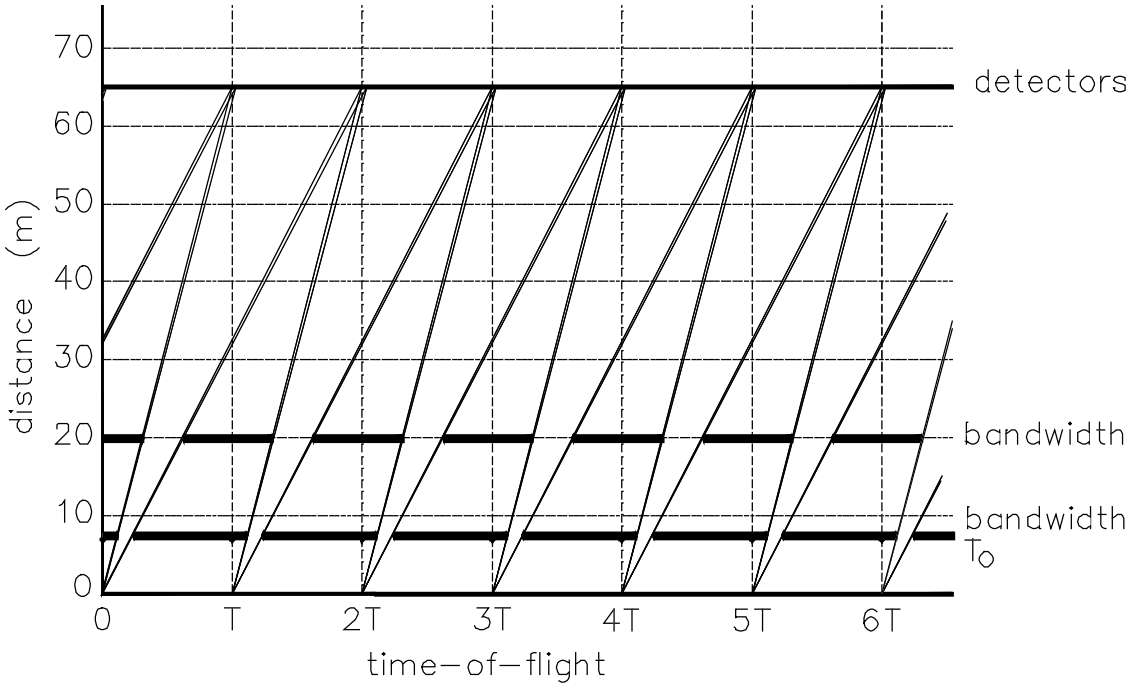

Fig. 16c

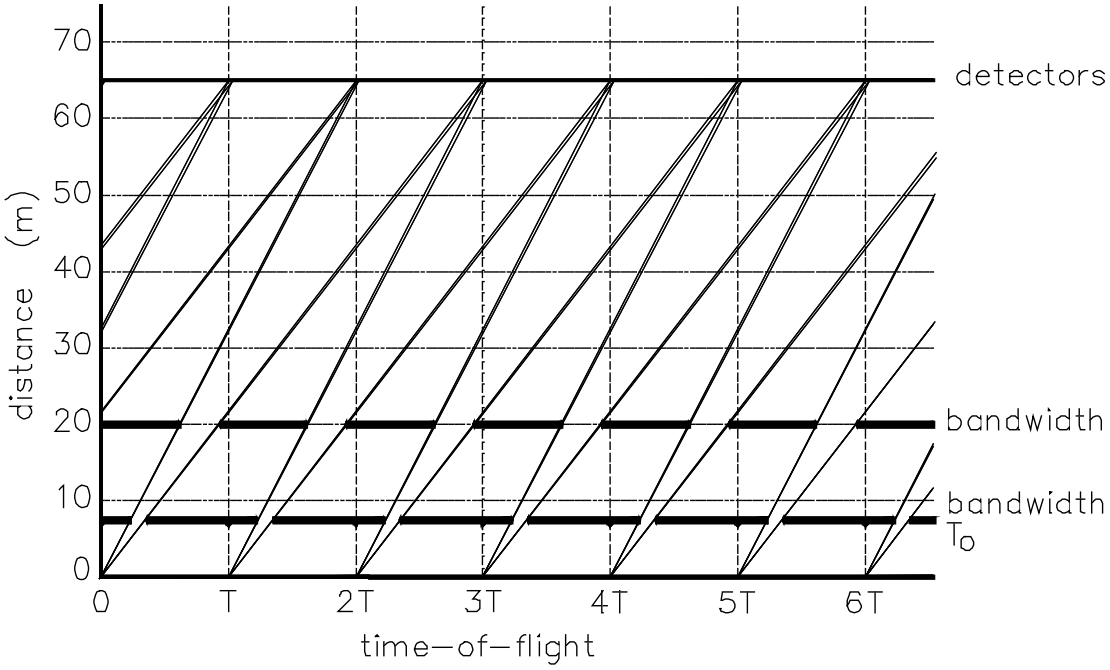

Fig. 16d

Figure 8. Timing diagram examples for POW-GEN3. a) frames 1-6 (0.18 to 6.09 Å); b) frame 1 (0.18 to 1.01 Å); c) frame 2 (1.05 to 2.03 Å); d) frame 3 (2.06 to 3.04 Å). The bandwidth lines indicate the boundaries of both the fully-open and fully-closed chopper conditions. Other options are easily produced with different chopper phasing and speed.

Table 2a. Opening and closing times for different chopper settings for POW-GEN3.

frame	1	2	3	4	5	6	1-2	1-3	1-4	1-5	1-6	4-6
t_{max} (μs)	16667	33333	50000	66667	83333	100000	33333	50000	66667	83333	100000	100000
T_0 freq (Hz)	60.0	60.0	60.0	60.0	60.0	60.0	60.0	60.0	60.0	60.0	60.0	60.0
T_0 Δt (μs)	159	159	159	159	159	159	159	159	159	159	159	159
BW1 freq (Hz)	60.0	60.0	60.0	60.0	60.0	60.0	30.0	20.0	15.0	12.0	10.0	20.0
BW1 Δt (μs)	159	159	159	159	159	159	318	477	637	796	955	477
BW2 freq (Hz)	60.0	60.0	60.0	60.0	60.0	60.0	30.0	20.0	15.0	12.0	10.0	20.0
BW2 Δt (μs)	159	159	159	159	159	159	318	477	637	796	955	477
t_{min} (μs)	1881	17184	33851	50517	67184	83851	1881	1881	1881	1881	1881	51552
T_0 t_c (μs)	0	16667	33333	50000	66667	83333						
T_0 t_{eo} (μs)	159	16826	33492	50159	66826	83492						
T_0 t_{sc} (μs)	16508	33174	49841	66508	83174							
BW1 t_{so} (μs)	58	1824	3747	5670	7593	9516	-101	-260	-420	-579	-738	5471
BW1 t_{eo} (μs)	217	1983	3906	5829	7752	9675	217	217	217	217	217	5948
BW1 t_{sc} (μs)	1923	3846	5769	7692	9615	11538	3846	5769	17692	9615	11538	11538
BW1 t_{ec} (μs)	2082	4005	5928	7851	9775	11698	4164	6247	18329	10411	12493	12016
BW2 t_{so} (μs)	420	5128	10256	15385	20513	25641	260	101	-58	-217	-376	15385
BW2 t_{eo} (μs)	579	5287	10416	15544	20672	25800	579	579	579	579	579	15862
BW2 t_{sc} (μs)	5128	10256	15385	20513	25641	30769	10256	15385	20513	25641	30769	30769
BW2 t_{ec} (μs)	5287	10416	15544	20672	25800	30928	10575	15862	21149	26437	31724	31247

T0 = t-zero chopper, BW1 = first bandwidth chopper, BW2 = second bandwidth chopper
f = frequency, Δt = time for chopper edge to sweep thru beam
so = start open; eo = end open; c = fully closed; sc = start close; ec = end close
This table assumes $\Delta t_{cl}=0$ for the T_0 chopper.

Table 2b. Accessible wavelengths for different chopper settings for POW-GEN3.

Frame N	1	2	3	4	5	6	1-2	1-3	1-4	1-5	1-6	4-6
t_{max} (μs)	16667	33333	50000	66667	83333	100000	33333	50000	66667	83333	100000	100000
T_0 freq (Hz)	60.0	60.0	60.0	60.0	60.0	60.0	60.0	60.0	60.0	60.0	60.0	60.0
T_0 Δλ (Å)	0.11	0.11	0.11	0.11	0.11	0.11	0.11	0.11	0.11	0.11	0.11	0.11
BW1 freq (Hz)	60.0	60.0	60.0	60.0	60.0	60.0	30.0	20.0	15.0	12.0	10.0	20.0
BW1 Δλ (Å)	0.08	0.08	0.08	0.08	0.08	0.08	0.17	0.25	0.34	0.42	0.50	0.25
BW2 freq (Hz)	60.0	60.0	60.0	60.0	60.0	60.0	30.0	20.0	15.0	12.0	10.0	20.0
BW2 Δλ (Å)	0.03	0.03	0.03	0.03	0.03	0.03	0.06	0.09	0.13	0.16	0.19	0.09
$\lambda_{inc\text{-}max}$ (Å)	1.01	2.03	3.04	4.06	5.07	6.09	2.03	3.04	4.06	5.07	6.09	6.09
$\lambda_{inc\text{-}min}$ (Å)	0.18	1.05	2.06	3.07	4.09	5.10	0.11	0.11	0.11	0.11	0.11	3.14
T_0 λ_c (Å)	0.00	11.99	23.97	35.96	47.94	59.93						
T_0 λ_{eo} (Å)	0.11	12.10	24.09	36.07	48.06	60.04						
T_0 λ_{sc} (Å)	11.87	23.86	35.84	47.83	59.82							
BW1 λ_{so} (Å)	0.03	0.96	1.98	2.99	4.00	5.02	-0.05	-0.14	-0.22	-0.31	-0.39	2.89
BW1 λ_{eo} (Å)	0.11	1.05	2.06	3.07	4.09	5.10	0.11	0.11	0.11	0.11	0.11	3.14
BW1 λ_{sc} (Å)	1.01	2.03	3.04	4.06	5.07	6.09	2.03	3.04	4.06	5.07	6.09	6.09
BW1 λ_{ec} (Å)	1.10	2.11	3.13	4.14	5.15	6.17	2.20	3.29	4.39	5.49	6.59	6.34
BW2 λ_{so} (Å)	0.08	1.01	2.03	3.04	4.06	5.07	0.05	0.02	-0.01	-0.04	-0.07	3.04
BW2 λ_{eo} (Å)	0.11	1.05	2.06	3.07	4.09	5.10	0.11	0.11	0.11	0.11	0.11	3.14
BW2 λ_{sc} (Å)	1.01	2.03	3.04	4.06	5.07	6.09	2.03	3.04	4.06	5.07	6.09	6.09
BW2 λ_{ec} (Å)	1.05	2.06	3.07	4.09	5.10	6.12	2.09	3.14	4.18	5.23	6.27	6.18

T0 = t-zero chopper, BW1 = first bandwidth chopper, BW2 = second bandwidth chopper
f = frequency, Δt = time for chopper edge to sweep thru beam
so = start open; eo = end open; c = fully closed; sc = start close; ec = end close
This table assumes Δt_{cl}=0 for the T_0 chopper.

3.2 Guide

The intensity on the sample is given by the intensity with no guide multiplied by the gain from the guide. The neutron guide system for POW-GEN3 was designed to permit the reduction of the incident beam divergence to the value available from natural collimation (i.e., horizontal collimation given by the ratio of the moderator size to the incident path length). This low incident divergence is required to give the best resolution for this instrument. This condition implies a horizontal gain of the guide of at most unity, and under this condition the intensity at the sample is independent of the guide width, provided the intensity is uniform across the moderator face and the requirements for full guide illumination are met.

This guide is curved to minimize the transmission of fast neutrons from the prompt pulses. Such guide curvature can introduce a wavelength-dependence of the effective beam position at the sample. Further studies will be required to determine the magnitude of this effect and to determine whether it can be reduced sufficiently by the introduction of a straight guide section after the curved section.

Monte Carlo simulations were used to obtain a more accurate estimate of the performance of the POW-GEN3 guide system. Parameters were those in Table 1 except as noted. For the simulations, neutrons were assumed to be emitted with equal probability from the entire moderator surface, and with equal probability within the angular range ±0.06 radians about the nominal beam direction. Since the critical angle for natural Ni at 10 Å is only 0.017 radians, this range of angular divergence was more than enough to include all neutrons that could be accepted by the POW-GEN3 guides. The same number of randomly generated initial neutron paths (1,000,000) was used for each 1-dimensional simulation, and total guide performance was obtained by comparing neutrons on sample with and without the guide for the corresponding simulations for the horizontal and vertical direction. For the vertical guide simulations, the guides were assumed to have reflectivity of 1.0 up to the critical angle θ_c for natural Ni, and a reflectivity of 0.88 from θ_c to $3\theta_c$, except as noted. Table 3 shows the simulation results.

Table 3a. Simulated horizontal guide gains for POW-GEN3 (no gap in guide)

L_{scat} (m)	L_{inc} (m)	W_{guide} (cm)	$G_{horiz}(\lambda=1)$	$G_{horiz}(\lambda=3)$	$G_{horiz}(\lambda=6)$	$G_{horiz}(\lambda=10)$
9	8	1.5	0.89	0.98	0.98	0.98
9	8	3.0	0.93	2.02	2.01	2.01
9	2.5	1.5	0.86	0.95	0.95	0.98
9	2.5	3.0	0.85	1.84	1.83	1.87
9	1	1.5	0.81	0.99	0.98	0.98
9	1	3.0	0.94	1.96	1.93	1.96
4	8	1.5	1.28	2.24	2.23	2.23
4	1	1.5	1.25	2.23	2.22	2.21
4	8	3.0	1.26	4.26	4.45	4.45
4	1	3.0	1.34	4.14	4.43	4.49

L_{inc} is the distance from the moderator to the start of the guide.
All calculations assume sample width of 1 cm.

Table 3b. Simulated vertical guide gains for POW-GEN3 (no gap in guide)

L_{scat} (m)	L_{inc} (m)	H_{guide} (cm)	$G_{vert}(\lambda=1)$	$G_{vert}(\lambda=3)$	$G_{vert}(\lambda=6)$	$G_{vert}(\lambda=10)$
1	2.5	6.0*	4.43	10.98	15.56	18.74
1	2.5	6.0	3.80	7.93	11.58	16.76
1	2.5	3.0	3.10	5.95	9.56	13.21
1	8	6.0*	4.38	6.81	7.51	7.53
1	8	6.0	3.89	6.06	7.51	7.53
1	8	3.0	3.29	5.66	7.37	7.37

L_{inc} is the distance from the moderator to the start of the guide.
All calculations assume sample height of 2 cm.
* Using effective super-mirror reflectivity of 0.95.

Preliminary Guide Conclusions

1. A 1.5 cm guide terminating 9 m from the sample gives roughly "natural" collimation
2. Any gains that can be achieved by making the guide wider can also be achieved by extending the guide closer to the sample
3. There is no point in extending the horizontal guide closer to the moderator than ~8 m
4. Some additional gains can be achieved at the longer wavelength by extending the vertical guide to within 2.5 m of the moderator – but the resulting angular divergences may be unacceptable in nearly all cases
5. For a 2 cm sample height, there is virtually no difference between a vertical guide 3 cm tall one 6 cm tall
6. For this guide design, there is not a strong dependence on the quality of the supermirror
7. There should be automatically insertable guide sections between ~9 m from the sample and ~1 m from the sample to allow trading resolution for intensity as needed

3.3 Detectors and Data Acquisition

The estimated instantaneous and time-averaged data rates per cm^2 are not particularly challenging. However, significant challenges arise in providing complete detector coverage over the complex curvature of the detector array. Providing an efficient means for readout of the $\sim 2.4\times10^5$ pixels will also be a challenge. Finally, development of the technology to provide the ~47 m^2 of detector arrays meeting these specifications at a reasonable cost will also be very important.

This instrument will also provide numerous challenges for the data acquisition system. The $\sim 2.4\times10^5$ pixels and 1 Å wavelength range will require $>10^9$ histogram channels to accommodate the full wavelength-angle data set. Efficient means of storing, accessing, and manipulating such data sets will be a must. However, handling the estimated time-averaged data rate of $<10^6$ counts/s should not be particularly challenging.

4 Discussion

Remaining Questions

Several questions must be answered before this instrument can be more fully optimized

What should be the refined performance specifications for the design of this instrument?

What is the optimal bandwidth?

How should the detector locus be optimized?

What is the optimal combination of out-of-plane detector coverage, sample height, and vertical guide gain?

What detector technology would permit cost-effective coverage of the desired detector locus and detector area?

How can the large data sets be handled?

Most of these questions require input from the broad user community. Some of these questions will be answered when the Monte Carlo simulation codes are more fully developed. Data from such simulations would be refined by the Rietveld method and the results compared with those from alternative instrument designs in order to assess and optimize the full potential of this third-generation instrument concept.

Required R&D

The areas indicated above that require R&D effort include:

improved simulation capabilities,

enhanced Rietveld refinement codes,

significantly improved detector technology, and

sophisticated data acquisition, storage, and handling systems.

References

[1] POW-GEN3 High-Resolution General Purpose Powder Diffractometer Conceptual Design Study, Doc. No. ES-1.1.8.2-6013-RE-A-00.